THE AMERICAN SOCIETY OF MECHANICAL ENGINEERS
345 E. 47th St., New York, N.Y. 10017

97-GT-519

The Aerodynamics of Trailing-Edge-Cooled Transonic Turbine Blades: Part 2 - Theoretical and Computational Approach

Mathias Deckers
Steam Turbine Development
Siemens Power Generation (KWU)
Mülheim / Ruhr, Germany

John D. Denton
Whittle Laboratory
University of Cambridge
Cambridge, United Kingdom

ABSTRACT

A theoretical and computational study into the aerodynamics of trailing-edge-cooled transonic turbine blades is described in this part of the paper. The theoretical study shows that, for unstaggered blades with coolant ejection, the base pressure and overall loss can be determined exactly by a simple control volume analysis. This theory suggests that a thick, cooled trailing edge with a wide slot can be more efficient than a thin, solid trailing edge. An existing time-marching finite volume method is adapted to calculate the transonic flow with trailing edge coolant ejection on a structured, quasi-orthogonal mesh. Good overall agreement between the present method, *inviscid* and viscous, and experimental evidence is obtained.

NOMENCLATURE

Roman and Greek Symbols

c_p	specific heat	sl	coolant slot width
C_m	coolant mass flow ratio	te	trailing edge thickness
C_{pb}	base pressure coefficient	T_0	stagnation temperature
C_{sl}	coolant slot coefficient	V	velocity
$\dot{m}$	mass flow	β	flow angle
M	Mach number	δ	bound layer thickness,
p	static pressure, pitch		deviation
p_0	stagnation pressure	δ^*	displacement thickness
$\overline{p}_{ss}$	avg suction surf pressure	γ	stagger angle
p_{b0}	base pressure($C_m = 0$)	θ	momentum thickness
s	blade pitch (spacing)	ρ	density

ξ kinetic energy loss coefficient (defined in Part 1)

Subscripts

1	main (flow)	c	coolant (flow)
2	mixed-out (flow)	is	isentropic
b	base	sl	slot

INTRODUCTION

So far, only little effort has been invested into developing methods of predicting the losses which occur in turbine blading with trailing edge coolant ejection. Nearly all of these methods fall into two main categories, i.e. analytical methods and Navier-Stokes methods.

The analytical methods are essentially based upon the theories developed by Stewart (1955) and Lieblein and Roudebush (1956) for solid blading which have been subsequently modified to allow for coolant ejection. The basic idea is to apply the global conservation equations between the trailing edge plane and an imaginary plane far downstream where the flow is regarded as being uniform and fully mixed out, e.g. Hartsel (1972), Prust (1972), Schobeiri (1989). Within the analysis the static pressure, primary flow angle and coolant flow angle are all presumed to be uniform across the trailing edge plane. This effectively means that the base pressure problem is circumvented and hence the importance of trailing edge loss is greatly underestimated, Xu (1985).

Very little work has yet been published that attempts to predict the detailed viscous flow field through turbine blade passages with trailing edge coolant ejection. In fact, it is only recently that research work aimed at developing numerical simulation programs to tackle this

Presented at the International Gas Turbine & Aeroengine Congress & Exhibition
Orlando, Florida — June 2–June 5, 1997

complex problem has started, e.g. Martelli *et al.* (1992), Michelassi *et al.* (1994). Considering the rapid developments in computer power together with the continuous improvements in computational fluid dynamics, these Navier-Stokes methods will undoubtedly become important in future.

This part of the paper involves a theoretical and computational investigation into the aerodynamics of trailing-edge-cooled transonic turbine blades. First, a control volume analysis is applied to a choked cascade of flat plates. The method is based upon that developed by Denton and Xu (1989), but this has been extended to allow for coolant ejection from the trailing edge base. Second, the development of a quasi-3D, explicit time-marching scheme for the calculation of transonic flow in the blade-to-blade plane is presented. To improve the accuracy of the solution a structured, quasi-orthogonal mesh is used. The effects of trailing edge coolant ejection are also considered. Results from *inviscid* and viscous predictions are given and compared with experimental data.

THEORETICAL METHOD

Description of the Theory

The cascade under consideration is illustrated in Fig. 1a. The control volume is delineated by the dashed line ABCDEFA. The control surfaces AB and CD are periodic boundaries with no net fluxes or pressure gradients across them. The theory assumes choked blade rows (but this is not unrealistic for high pressure turbines which often operate at choked conditions) and constant area, adiabatic mixing behind the trailing edge. Blade surface and coolant flow boundary layers are also included in the analysis.

Since the main flow is assumed to be choked at the throat, the mass flow rate is fixed and given by

$$\frac{\dot{m}_1\sqrt{c_p T_{01}}}{(s\cos\gamma - te - \delta^*)p_{01}} = F(M_1 = 1) = const. \qquad (1)$$

whereas the following mass flow function

$$\frac{\dot{m}_2\sqrt{c_p T_{02}}}{s\cos(\gamma-\delta)p_{02}} = F(M_2) \qquad (2)$$

is pertinent to the uniform mixed-out flow far downstream of the cascade. Assuming adiabatic mixing, the energy equation enables us to determine T_{02}:

$$\dot{m}_2 T_{02} = \dot{m}_1 T_{01} + \dot{m}_c T_{0c} \quad . \qquad (3)$$

The combination of Eqs. (1) and (2) leads to the mixed-out stagnation pressure, p_{02}, namely

$$\frac{p_{02}}{p_{01}} = \frac{F(M_1=1)}{F(M_2)}\,\frac{s\cos\gamma - te - \delta^*}{s\cos(\gamma-\delta)}\,\frac{\dot{m}_2}{\dot{m}_1}\sqrt{\frac{T_{02}}{T_{01}}} \qquad (4)$$

Examination of Eq. (4) shows that the ejection of coolant and the associated increase in the mass flow rate tends to increase the mixed-out stagnation pressure but the reduction in stagnation temperature will partially compensate this effect.

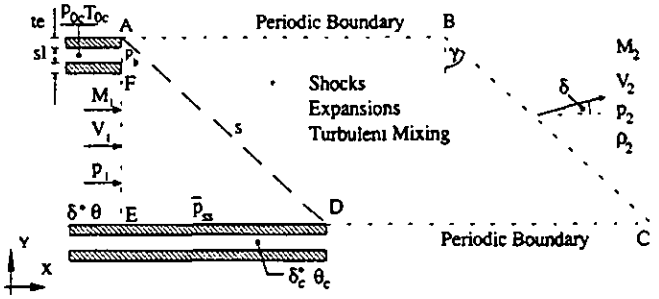

Fig. 1a: Control Volume for Global Theory; Staggered Blades

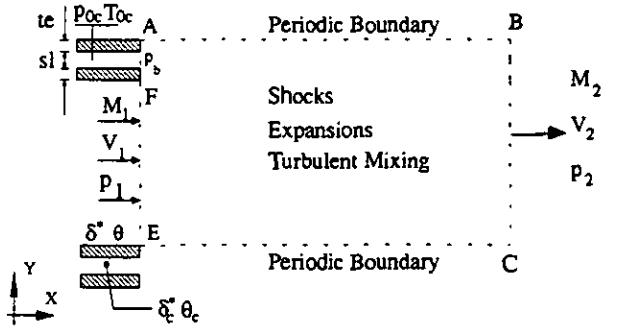

Fig. 1b: Control Volume for Global Theory; Unstaggered Blades

The x-momentum equation[1] is given by

$$\dot{m}_1 V_1 - \rho_1 V_1^2\theta + \dot{m}_c V_c - \rho_c V_c^2\theta_c + p_1(s\cos\gamma - te) + p_b\,te = \dot{m}_2 V_2\cos\delta + p_2 s\cos\gamma \qquad (5)$$

and similarly the y-momentum equation

$$\bar{p}_{ss}\,s\sin\gamma = p_2 s\sin\gamma + \dot{m}_2 V_2\sin\delta \qquad (6)$$

where $\bar{p}_{ss}$ is the average pressure acting on the suction surface downstream of the throat. It can be seen from Eqs. (4) and (5) that the inclusion of boundary layers via combined values for δ^* and θ acts to increase the base pressure, but the global loss is also increased.

Inspection of Eqs. (1) - (6) shows that if the cascade geometry is given and the main and coolant flow stagnation conditions together with the exit Mach number are specified, a further relationship is necessary to close the system of equations, e.g. $\bar{p}_{ss} = F(p_b, p_2)$. Provided that such a relationship can be postulated the control volume theory should exactly determine the base pressure and its associated loss without the need to include any viscous effects downstream of the trailing edge. Although, the detailed flow field will undoubtedly be characterised by viscous effects their magnitude is determined by the

[1] It should be pointed out that the Mach number of the coolant at the exit of the slot, M_c, is artificially restricted to unity, implying that the coolant passage is converging. In this case, the base pressure is assumed to act at the two partial bases only, and the coolant static pressure at the exit is determined from the choking condition.

global conservation equations and boundary conditions, Denton and Xu (1989).

However, the predictions were found to be extremely sensitive to the assumption for $\bar{p}_{ss}$. The simplest approximation is probably to assume that $\bar{p}_{ss} = p_2$, which, according to Eq. (6), implies that the deviation, δ, is zero, Denton (1993). In this case, the base pressure and loss become independent of the stagger angle and so the results for a staggered cascade will be the same as for an unstaggered cascade with the same trailing edge blockage. An alternative approach is to assume that $\bar{p}_{ss} = p_1$, Stewart (1955), in which case the deviation is negative. In practice, the average suction surface pressure is likely to lie somewhere between these two assumptions. The cascade tests (Part 1) have shown that the measured difference between the average suction surface pressure, $\bar{p}_{ss}$, and the exit static pressure, p_2, was found to be less than 5% for all exit Mach numbers tested and, hence, the first assumption appears to be fairly realistic. Therefore, only unstaggered trailing edges will be considered here.

Results for Unstaggered Blades with Trailing Edge Ejection

The global theory can be readily applied to an unstaggered cascade of flat plates by simply setting the stagger angle, γ, equal to zero. The problem becomes one-dimensional (Fig. 1b) and the global conservation equations can be solved to exactly predict the base pressure and overall loss for a specified exit Mach number.

Note, the conservation equations have to be solved iteratively for the calculation of the base pressure and mixed-out loss when coolant flow is ejected from the trailing edge base. The parameters[2] used to characterise the coolant flow are the ratio of the coolant stagnation pressure, p_{0c}, to the base pressure in absence of coolant ejection, p_{b0}, and the coolant mass flow ratio, $C_m = \dot{m}_c / \dot{m}_1$.

Influence of Coolant Stagnation Pressure Ratio and Slot Width

In Fig. 2, the variation of the base pressure coefficient, C_{pb}, with coolant flow rate, characterised by (p_{0c} / p_{b0}), is plotted. The calculations were performed for an isentropic exit Mach number of $M_{2is} = 0.8$ [3] and a trailing edge blockage of 20%. Main flow and coolant flow were assumed to mix at the same stagnation temperature, so $T_{0c} = T_{01}$. Boundary layer effects were not included. The four curves shown refer to different values of the coolant slot coefficient, $C_{sl} = sl / te$.

It can be seen that a substantial increase in base pressure is achieved due to the ejection of coolant but this effect is less pronounced with decreasing slot width. Maximum base pressure is obtained for the widest slot ($C_{sl} = 0.5$) and an ejection pressure ratio of $p_{0c} / p_{b0} = 2.2$ ($C_m = 7\%$).

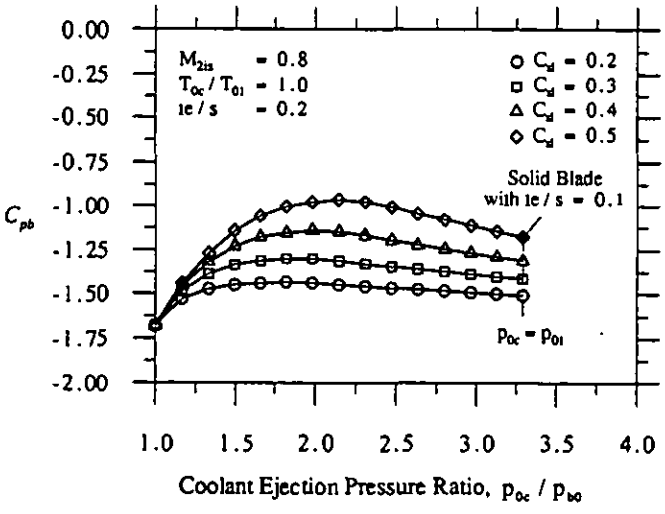

Fig. 2: Variation of Base Pressure Coefficient with Coolant Flow

The corresponding variations of the kinetic energy loss coefficient with ejection pressure ratio is presented in Fig. 3. It can be seen that trailing edge ejection reduces considerably the loss coefficient with increasing coolant flow but for high bleed rates, the mixed-out loss starts to rise again. This is because the coolant flow approaches choking at high ejection pressure ratios and, hence, starts to behave similarly to the main flow. The coolant expands supersonically around the trailing edge corner and a fully supersonic base triangle is established at each partial base with a corresponding reduction in base pressure, Fig. 2. As a consequence, a solid blade with 10% blockage and a cooled blade with 20% blockage and slot coefficient $C_{sl} = 0.5$ both produce the same base pressure and loss. This is highlighted in Figs. 2 and 3.

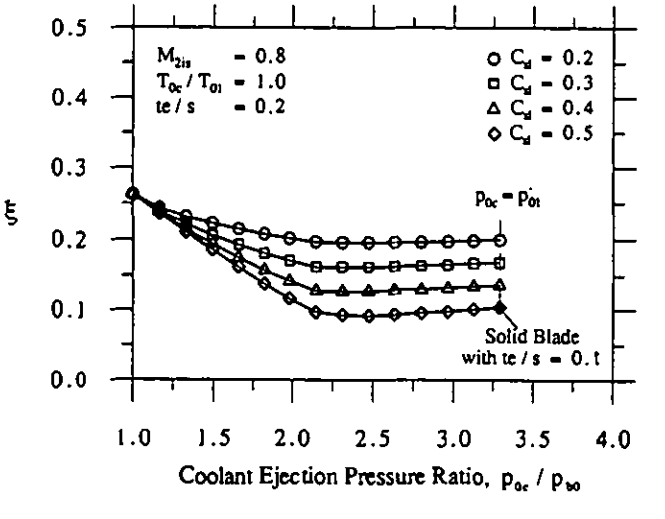

Fig. 3: Variation of Kinetic Energy Loss Coefficient with Coolant Flow

[2] Alternatively, the coolant mass flux ratio ($\rho_c V_c / \rho_1 V_1$) is used by several investigators to characterise the coolant flow, e.g. Schobeiri (1989). Although the coolant parameter will affect the mechanism of dissipation the control volume analysis shows that it does not directly affect the overall dissipation.

[3] It should be mentioned that in order to arrive at a solution for an *isentropic* exit Mach number, M_{2is}, the *true* mixed-out Mach number, M_2, is iteratively changed until the specified value for M_{2is} has been achieved.

The calculations show that minimum loss and maximum base pressure occur at different coolant flow rates, the latter being achieved with less bleed. The theory confirms, therefore, the results from the model tests (Part 1). Both, minimum loss and maximum base pressure, are obtained well before the coolant stagnation pressure equals the main flow stagnation pressure ($p_{0c} = p_{01}$) which, as indicated in Figs. 2 and 3, is the last point given on each of the curves. The predictions suggest that a cooled trailing edge, with thickness te, operating at optimum coolant flow rate, is more efficient than a solid trailing edge with thickness ($te - sl$), where sl is the coolant slot width, Fig. 3.

Influence of Coolant Stagnation Temperature Ratio

The control volume analysis can be employed to theoretically study the effect of the coolant stagnation temperature ratio. In Figs. 4 and 5, the results are plotted against coolant ejection pressure ratio for an isentropic exit Mach number of $M_{2is} = 0.8$. Again, boundary layers were not included in the analysis. The predictions shown correspond to different coolant stagnation temperature ratios, varying between 0.6 and 1.0 .

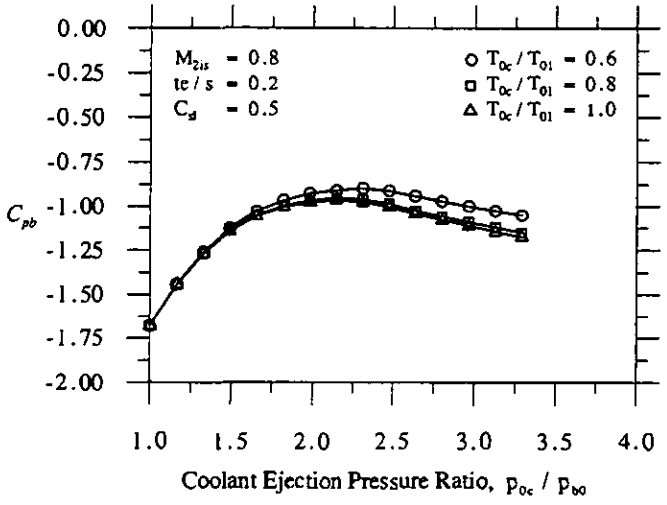

Fig. 4: Influence of Coolant Stagnation Temperature Ratio on Base Pressure Coefficient

The predictions indicate generally that the effect of the stagnation temperature ratio upon the base pressure and loss appears to be insignificant, and, hence, confirm the findings observed in the experiments discussed in Part 1. However, the data suggest that a reduction in temperature ratio may cause a slight increase in base pressure coefficient at high ejection rates in particular for $T_{0c} / T_{01} = 0.6$; the biggest improvement being achieved for maximum coolant flow, i.e. $p_{0c} / p_{01} = 1$. The impact of (T_{0c} / T_{01}) on the kinetic energy loss coefficient can be seen to be very small, Fig. 5, and appears to be greatest for coolant ejection rates which correspond to minimum loss. However, the influence is reduced at higher flow rates than this and is negligible at the maximum coolant flow rate because the coolant chokes at high ejection rates regardless of the coolant temperature ratio. When choking occurs the coolant momentum flux ($\rho_c V_c^2$) is determined by the choking condition and, hence, it is not affected by the temperature ratio.

It must be remembered that, due to an increased coolant density at lower temperatures, the coolant mass flow increases with decreasing coolant temperature for a given coolant ejection pressure ratio (p_{0c} / p_{01}). Therefore, the small changes encountered are believed to have been brought about mainly by the associated addition in mass flow.

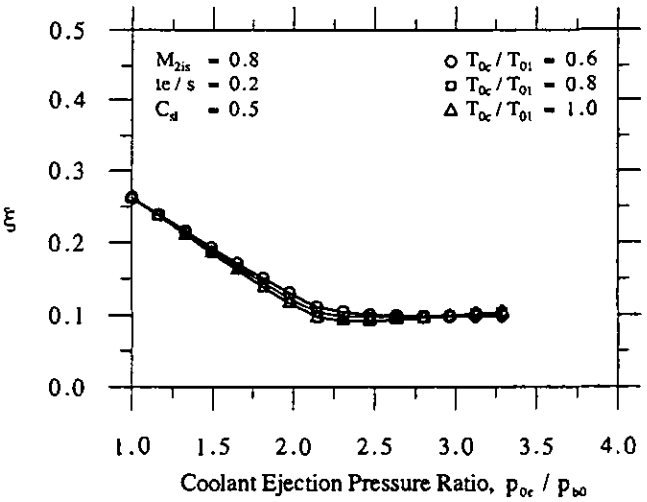

Fig. 5: Influence of Coolant Stagnation Temperature Ratio on Kinetic Energy Loss Coefficient

Comparison with Measurements

Provided that the boundary conditions are correctly specified, the simple control volume analysis as introduced above should exactly predict the base pressure and loss of an unstaggered blade regardless of whether or not coolant is ejected from the trailing edge base. To confirm this hypothesis, two base pressure and loss measurements acquired within the test program presented in Part I of this paper are compared with predictions obtained by the present theory. The results are shown in Figs. 6 and 7.

In Fig. 6a, the base pressure variation as a function of coolant flow rate is plotted for an exit Mach number of $M_{2is} = 0.85$, the isentropic test condition. In order to match the boundary conditions to be applied in the theory with those during testing, the mixed-out exit Mach number obtained from the experiments was specified in the calculation. Blade surface boundary layers were accounted for by means of combined integral parameters as measured within the experiments, typical values being $\delta^* = 0.7mm$ and $\theta = 0.5mm$. The (upper) dashed line in Fig. 6a represents the prediction obtained from the analysis. As shown, the theory tends to over-predict the base pressure increase due to coolant ejection. This is thought to be caused by the neglect of the coolant flow boundary layers. In order to check this assumption, coolant boundary layers have been incorporated into the analysis. The (lower) solid curve shows a prediction which accounts for an ejection velocity profile as a result of viscous interactions between coolant and channel wall. As a first approximation, a parabolic velocity distribution

was assumed as is commonly used for incompressible, laminar flow through a straight channel, Schlichting (1968). In doing so, coolant boundary layer integral parameters can be determined from the specified geometry, i.e. $\delta_c^* = sl/3$ and $\theta_c = 2sl/15$. As shown in Fig. 6a, the agreement between experiment and theory is very much improved. In fact, for coolant flow rates up to $p_{0c}/p_{b0} = 1.75$, the values are almost identical. However, the agreement can be seen to deteriorate as the bleed rate is increased further. The conclusions drawn above suggest that this is caused by mismatched boundary conditions between theory and experiment. The coolant flow in the slot, for instance, was found to become turbulent at high ejection pressure ratios.

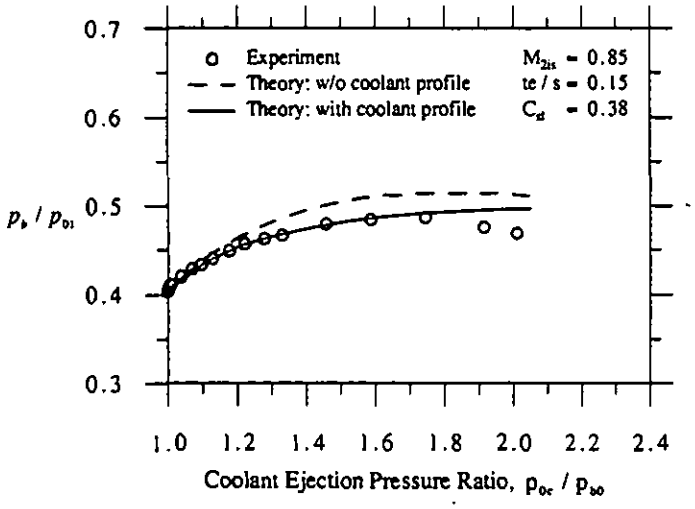

Fig. 6a: Predicted and Measured Base Pressures ($M_{2is} = 0.85$)

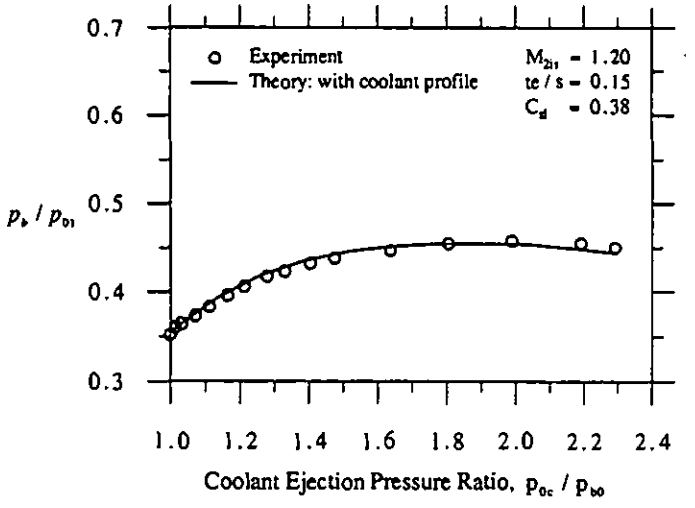

Fig. 6b: Predicted and Measured Base Pressures ($M_{2is} = 1.20$)

Figure 6b shows a comparison between predicted and measured base pressures versus coolant flow rate for an isentropic exit Mach number of $M_{2is} = 1.2$. Main and coolant flow boundary layers were included in the prediction and the agreement was found to be almost exact for all bleed rates.

The corresponding variations of the kinetic energy loss coefficient with coolant flow is plotted for $M_{2is} = 0.85$ and $M_{2is} = 1.2$ in Figs. 7a and 7b, respectively. The overall agreement between theoretical and experimental results can be seen to be good. There is, nevertheless, some discrepancy evident at zero and low coolant flow rates ($p_{0c} / p_{b0} < 1.1$). Since the base pressure was shown to be predicted correctly, Fig. 6, no convincing reasons can be given for this disagreement at low coolant ejection rates. However, the discrepancy is thought of being caused partly by the neglect of the so-called "cavity effect" which cannot be modelled properly in the analysis. In fact, the theory would say that it cannot exist in two-dimensional flow.

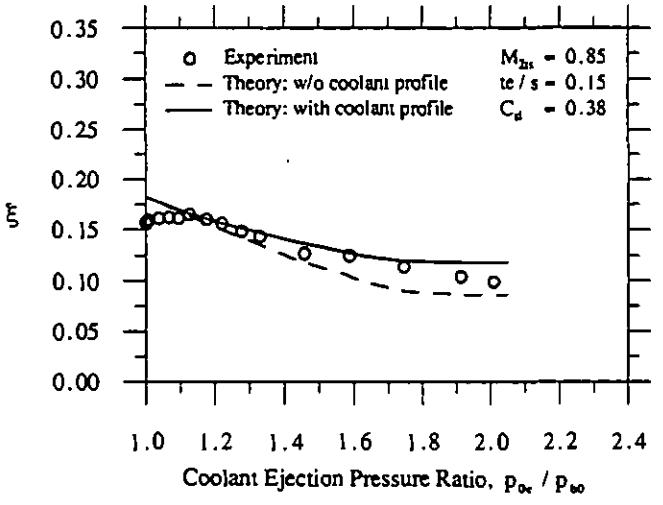

Fig. 7a: Predicted and Measured Variation of Kinetic Energy Loss Coefficient ($M_{2is} = 0.85$)

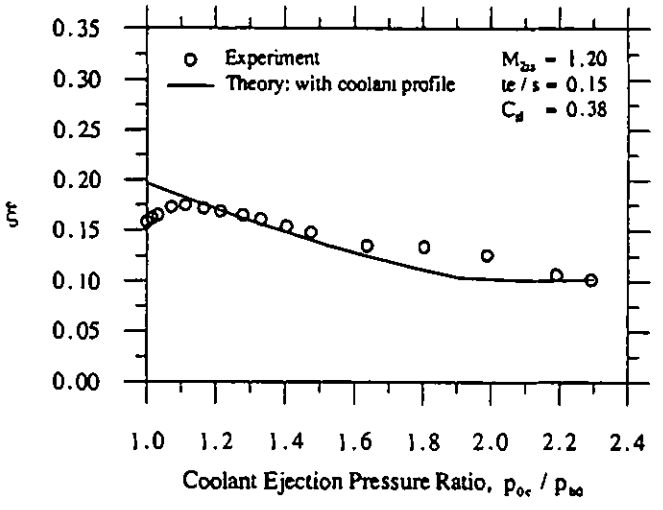

Fig. 7b: Predicted and Measured Variation of Kinetic Energy Loss Coefficient ($M_{2is} = 1.20$)

COMPUTATIONAL METHOD

Description of the Numerical Algorithm

Computational Method

The computational method employed here is a quasi-3D, explicit time-marching technique which numerically integrates the Navier-Stokes equations in finite volume form. The code is based upon that developed by Denton (1982), but this now incorporates the Ni (1989) differencing scheme. The integration method is second-order accurate in time and space and determines the corrections of the flow properties by so-called "distribution formulae" in the non-overlapping control volumes. To reduce the computational time required to arrive at a converged solution, two convergence acceleration techniques are implemented: single level multi-gridding and non-uniform time stepping. It can be shown that for a steady, adiabatic, isenthalpic flow with a Prandtl number of unity the shear work terms and the heat flow terms in the energy equation cancel, Denton (1986). Therefore, the total enthalpy is constant and the energy equation can be eliminated from the solution procedure. This is done for the sake of simplicity and to save CPU time. Artificial dissipation is necessary to ensure stability of captured shocks and reduce numerical oscillations around them. Explicit second and fourth order numerical smoothing of the dependent variables is therefore used but is kept at a low level, a typical value for the smoothing factor being *0.5%* in transonic flow with shock waves.

The code can be employed for both *inviscid* and viscous calculations. In case an *inviscid* solution is desired, the viscous flux terms are simply set equal to zero and the governing equations reduce to the Euler equations. The inclusion of viscous effects will allow boundary layers to develop along the blade surfaces and will allow turbulent mixing (instead of numerical mixing due to artificial viscosity) to take place in the highly viscous base region and wake. The effect of the blade boundary layers is twofold: they reduce the mass and momentum flows, and they change the static pressure distribution, on the suction surface of the blade mainly due to a shock wave-boundary layer interaction.

Although they are in principal capable of true predictions these viscous solvers suffer from the lack of realistic transition and turbulence models. For the sake of simplicity, the Prandtl mixing length formulation is employed in the present program. The mixing length is assumed to be proportional to the distance normal to the wall near the blade surface, but it is limited empirically at a prescribed distance of 10% of the blade pitch from the surface. Downstream of the blade row, the mixing length is held constant at a specified value of 5% of the blade pitch whilst, upstream of the leading edge, turbulence effects on the mean velocity field are not considered. A simple transition model as suggested by Baldwin and Lomax (1978) is also implemented into the program. However, for all the predictions to be presented below transition is forced to occur at the blades' leading edge.

In order to reduce grid resolution requirements in the near-blade region, a slip model of flow on the boundaries is used together with the log law wall function to determine the shear stress at the blade surface. However, instabilities were encountered at the position where the shock wave interacts with the boundary layer. Scaling the skin friction by a factor of 0.7 was found to stabilise the scheme. Although this approach is somewhat *ad hoc* the use of a wall function, which is based upon an assumption of an incompressible, equilibrium boundary layer, is unlikely to be very accurate in the region of the interaction.

A Quasi-Orthogonal Computational Mesh

The flow through modern, high-pressure turbine blading is characterised by considerable turning and strong deviation from the axial direction. A discretisation using a standard H-mesh will produce highly distorted control volumes which leads to high rates of shear and to a detrimental effect on the accuracy of the solution, Turner *et al.* (1993). This can be particularly troublesome in the trailing edge region of a transonic turbine blade with high exit angle where a standard H-mesh exhibits considerable regions of shear. As a consequence, the trailing edge shock is smeared over many grid-points leading to an inaccurate prediction of the suction surface pressure distribution.

In the present work, a standard H-type grid is modified to become a structured, nearly orthogonal computational mesh. Special attention is drawn towards an improved description of the wake and the imposition of periodic boundary conditions. The computational mesh to be described here can be looked at as a combination of a standard H-type mesh and a quasi-orthogonal mesh as shown in Fig. 8. The grid-lines are non-uniformly spaced in both directions in order to improve leading and trailing edge resolution and to capture the boundary layers on the blade surface. Downstream of the throat, both the inclination and axial spacing of the pitchwise grid-lines are kept constant which ensures a point-to-point grid correspondence to facilitate the enforcement of periodicity, Fig. 8. Additional mesh originating from the trailing edge base is introduced to improve the description of the wake. Figure 8 demonstrates that the present mesh exhibits very little shear and nearly orthogonal grid-lines[4].

Boundary Conditions

The theory of characteristics tells us that for a flow with a subsonic axial velocity component three boundary conditions have to be imposed at the inlet plane (e.g. p_{01}, T_{01}, β_1) and one condition at the outlet plane (e.g. p_2). Along the blade surface, including the trailing edge base or part of it in the case when trailing edge coolant ejection is simulated, an impermeability condition is imposed by setting the mass flux across the surface equal to zero. Upstream and downstream of the blade row periodicity is applied on corresponding grid-nodes along the bounding pseudo streamlines, Fig. 8. Note, the downstream boundary is made up of a pseudo streamline *AB* and a pitchwise grid-line *BC*. Both of which are treated as outflow boundaries so that the static pressure is held constant along *AB* and *BC*. Within the present study no difficulties have been encountered in treating the exit boundary in this way.

[4] Within the present study, no attempt has been made to improve the mesh resolution at the blade leading edge. The amount of false entropy generation in this region is believed to have a negligible effect upon trailing edge loss, and, at worst, should produce a systematic error in all the predictions.

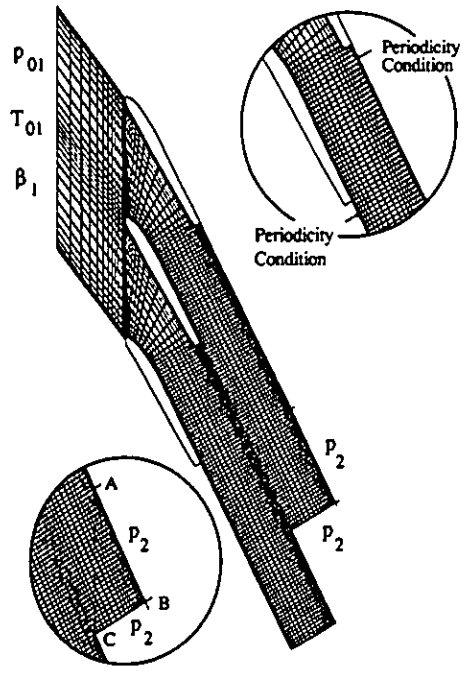

Fig. 8: Computational Mesh

The Inclusion of Trailing Edge Coolant Ejection

The time-marching program has been written to allow coolant to be ejected from a slot in the trailing edge base. The coolant is considered as a source of mass, momentum and energy and must therefore be included in the flux balance of the control volumes adjacent to the ejection location. As a consequence, the solid wall boundary condition is discarded at grid-points along the discharge slot and replaced with appropriate coolant boundary conditions for the stagnation pressure, p_{0c}, stagnation temperature, T_{0c}, and ejection angle, β_c. In order to obtain a more realistic coolant velocity profile, a parabolic stagnation pressure variation across the slot is prescribed. (Strictly speaking, this assumption of a laminar coolant velocity profile was justified only for low coolant flow rates.) The coolant stagnation temperature and angle both are assumed to be constant along the slot[5]. In order to identify the control volumes involved the coolant slot width and location must also be specified. A more detailed description of the numerical method can be found in Deckers (1996).

Computational Results and Comparison with Experiments

The simple global theory has shown that, if the average suction surface pressure downstream of the throat can be predicted accurately, the base pressure and overall loss can be exactly determined without the inclusion of any viscous effects downstream of the throat. It is for this reason that finite volume Euler solvers which do conserve mass, momentum and energy should predict the overall loss reasonably despite the inevitable smearing of expansion and shock waves. However, from the turbine designer's point of view, a knowledge of the absolute loss level is important, and it must be recognised that a solution of the full Navier-Stokes equations will ultimately to be sought.

In this section, results from *inviscid* and viscous calculations are presented and compared with experimental evidence presented in Part 1 of this paper. In order to ease comparisons, the resolution of the computational mesh and spacing near the wall was chosen such that the same mesh could be used for both types of calculations. The mesh is made up of 181 points in the streamwise direction, 41 in the pitchwise direction plus a further 12 grid-lines originating from the base. It was kept unchanged throughout the study. The smoothing factors were adjusted such that for the entire Mach number and coolant flow range the same values could be used. They were chosen to be 0.6% for *inviscid* predictions whilst 0.5% was employed for the viscous calculations.

Blades with Solid Trailing Edges

In the following, results obtained from calculations on solid blades without coolant ejection are presented. A comparison between an *inviscid* and viscous prediction is plotted in Fig. 9 in terms of contours of Mach number ($M_{2is} = 1.15$). Generally, the solutions have captured all the flow features (incl. expansions, shocks and their reflections) well without excessive numerical smearing. In reality, the flow within the base triangle is highly viscous and so the details of the predicted base flow obtained from the *inviscid* calculation are obviously incorrect. However, the shape of the triangle is determined by *inviscid* effects and can be predicted, for example, by the method of characteristics. The viscous calculation predicts a strong shock wave-boundary layer interaction which, in turn, leads to a thickening of the boundary layer.

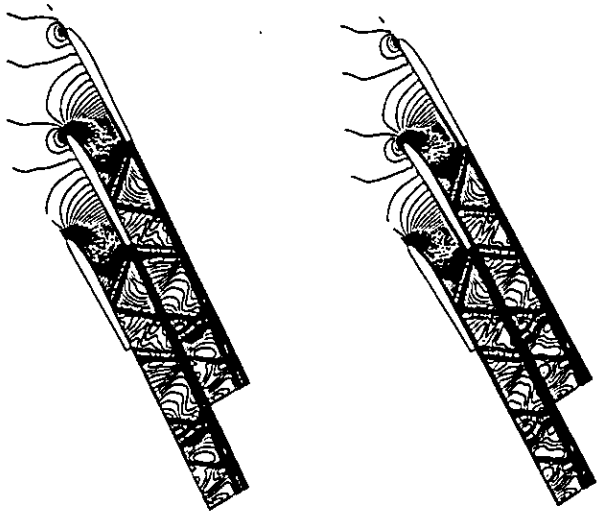

a) *Inviscid* Calculation b) Viscous Calculation

Fig. 9: Contours of Mach Number ($M_{2is} = 1.15$)

[5] It should be noted that since the energy equation has been excluded from the solution procedure only moderate differences between the mainflow and coolant stagnation temperatures can be dealt with. However, no attempt has been made to include the stagnation temperature ratio in the numerical study.

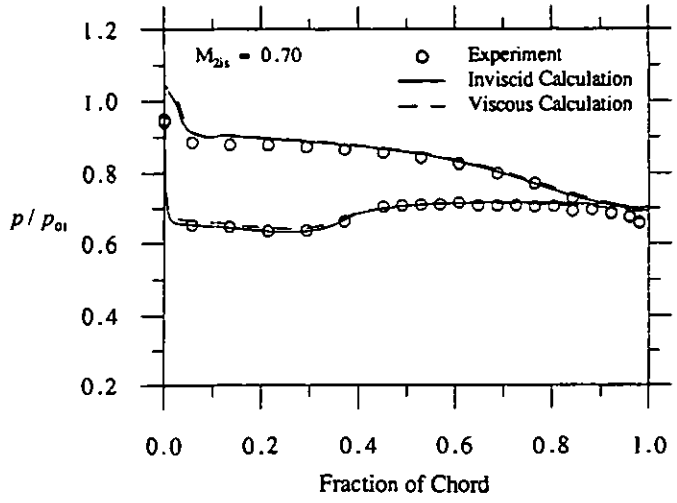

Fig. 10a: Surface Static Pressure Variation ($M_{2is} = 0.7$)

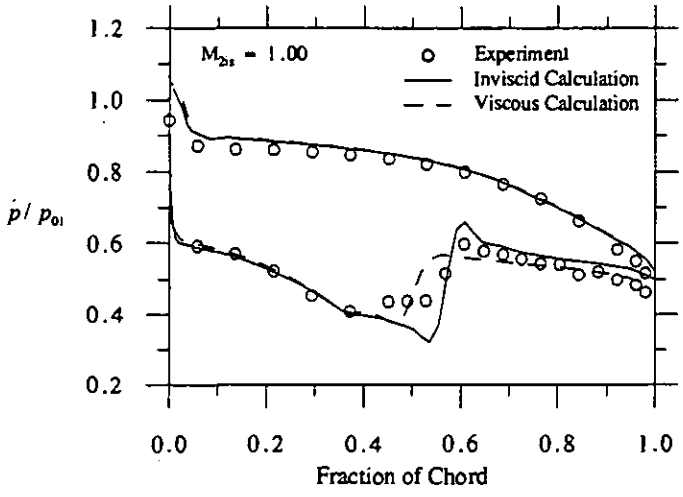

Fig. 10b: Surface Static Pressure Variation ($M_{2is} = 1.0$)

Figure 10 shows a comparison of the predicted and measured surface static pressure distributions for three exit Mach numbers. The disagreement at the leading edge of the pressure surface is thought to be caused by numerical errors arising from the poor modelling of the leading edge flow due to a course grid spacing. If the grid was refined then the results obtained were far more realistic. The rear part of the pressure surface, however, is generally fairly well predicted.

The agreement on the suction surface between *inviscid* predictions and experimental evidence is compromised by the fact that the calculation ignores blade surface boundary layers and their interaction with shock waves (Fig. 10). However, the predicted shock locations agree reasonably well with the test data. The discrepancy between predictions and measurements was found to be largest for $M_{2is} = 1.0$; most likely due to a strong shock-boundary layer interaction. The reasons for these discrepancies are numerical errors in the calculation, inaccurate modelling of the trailing edge flow and, most importantly, the neglect of viscous effects.

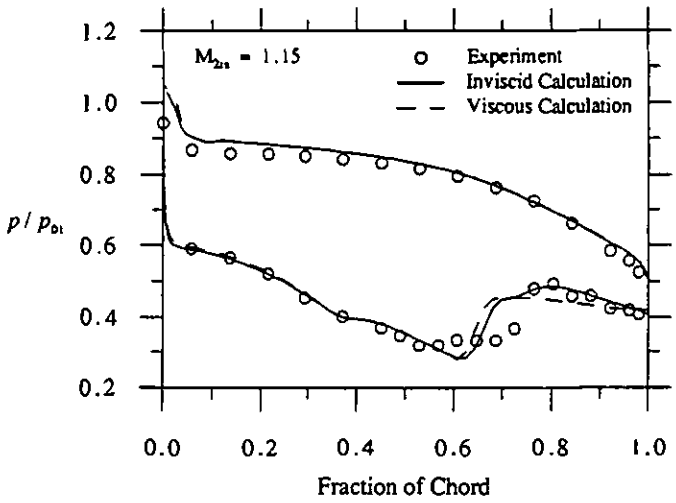

Fig. 10c: Surface Static Pressure Variation ($M_{2is} = 1.15$)

The viscous solver predicts the shock to be located further upstream when compared to the *inviscid* calculations (Fig. 10). Hence, better agreement is achieved in terms of shock location and pressure rise. However, the predictions generally suffer from the fact that the viscous time-marching method failed to predict the small separation bubble present at the position of the shock wave-boundary layer interaction seen in the test data, Deckers (1996). Therefore, the computed pressure rise is produced by a single shock wave, the trailing edge shock, whilst the experimental pressure rise is caused by a combination of both the incident and the re-attachment shock. There are two main reasons for this lack of accuracy. Firstly, the actual boundary layer in the cascade tests is likely to be laminar on the suction surface up to the position where the shock interacts with the boundary layer whilst a turbulent boundary layer over the entire surface length is assumed in the calculation. It is well known that a turbulent boundary layer is generally more able to withstand a high pressure rise, e.g. imposed by a shock wave, without separation. This may cause the calculated boundary layer to remain attached at the position of interaction. Secondly, it should be remembered that a very simple algebraic turbulence model is used which, strictly speaking, is applicable only to "simple" two-dimensional shear flows with "weak" pressure gradients, Lakshminarayana (1991).

A comparison between the predicted and measured base pressure variation[6], p_b / p_{01} , with isentropic exit Mach number, M_{2is} , is plotted in Fig. 11. At subsonic exit flow conditions with $M_{2is} \leq 0.8$, the agreement is very good but with increasing Mach number the rate of decrease in base pressure is under-predicted. Hence, the calculations produce higher base pressure values for all outlet Mach numbers at which the flow in the passage is choked ($M_{2is} \geq 0.9$). The largest discrepancy is found for Mach numbers of about unity. The errors are

[6] It should be noted that in both cases an average value is shown. The experimentally determined base pressure is the arithmetic mean of the two static pressures measured at the trailing edge base (Part 1). Similarly, the calculated value is the arithmetic mean of the predicted static pressures along the base.

due to the incorrect average pressure on the suction surface which in turn is due to the inability to predict (correctly) the shock-boundary layer interaction. The viscous calculation predicts a lower rate of decrease in base pressure compared to that produced by the *inviscid* method and so the Euler solver gives a better agreement. However, both methods predict the overall trend of the variation of base pressure with exit Mach number remarkably well.

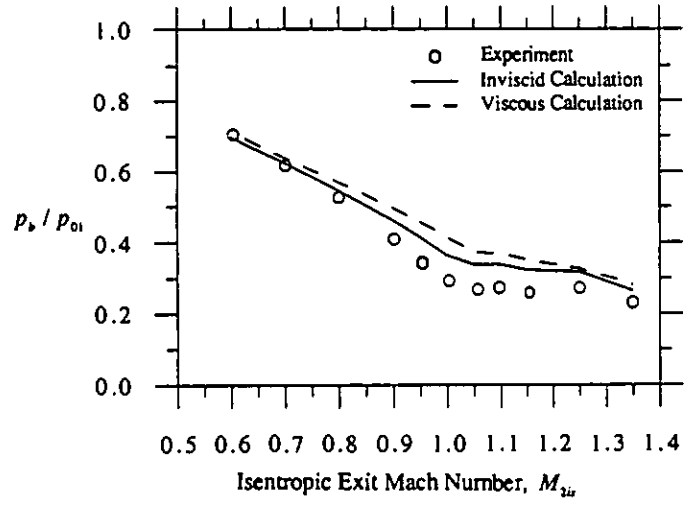

Fig. 11: Predicted and Measured Variation of Base Pressure

The calculated and measured kinetic energy loss coefficient[7], ξ, as a function of isentropic exit Mach number, M_{2is}, is compared in Fig. 12. As expected, the *inviscid* time-marching method predicts lower losses over the entire Mach number range. In the subsonic flow regime ($M_{2is} \leq 0.8$) the computed loss is produced by the action of numerical viscosity especially at the blades' leading and trailing edges where large velocity gradients exist whilst the measured loss is caused by a combination of blade surface boundary layers and subsonic base drag. The agreement between predicted and measured loss (and base pressure) in this Mach number range is therefore rather fortuitous. For choked flow ($M_{2is} \geq 0.9$), however, the variation in overall loss is caused by a change in trailing edge loss in both the calculations and the measurements. This, as was shown by the control volume analysis, can be explained using global arguments. The overall trend of the variation of predicted loss coefficient with exit Mach number compares very well with the experimental data indicating that the mechanisms involved can be explained by *inviscid* means. The absolute level is nevertheless influenced by viscous effects especially at Mach numbers around unity where a strong shock-boundary layer interaction is observed. Hence, it is not surprising to find a large disagreement in loss at $M_{2is} \approx 1$.

[7] The blade performance is described in a similar way to that used in the experiments (Part 1) and is obtained from a mixing calculation between the exit plane and a hypothetical plane far downstream where the flow is assumed to be fully mixed-out, Amecke (1970). In doing so, flow quantities along the dashed line AC in Fig. 8 are determined by linear interpolation between neighbouring grid-points to be used as input to the mixing calculation.

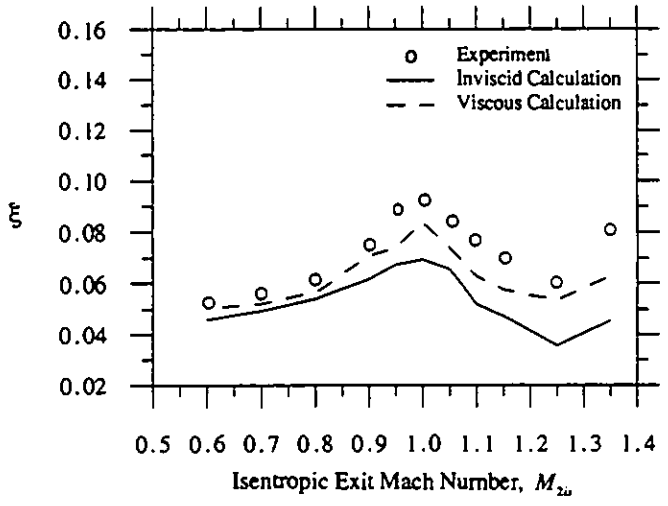

Fig. 12: Predicted and Measured Variation of Loss Coefficient

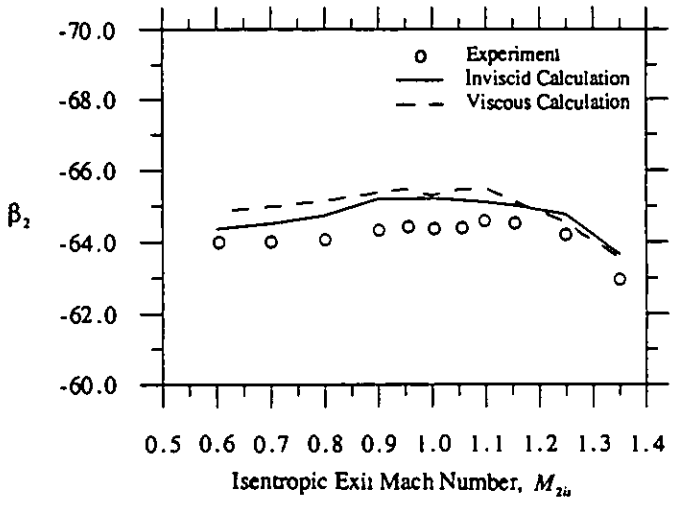

Fig. 13: Predicted and Measured Variation of Exit Flow Angle

The viscous solver computes a loss variation which follows closely the trends of the measured loss but the values are found to be somewhat low. It has to be borne in mind, however, that since the trailing edge loss is under-estimated, meaning that the base pressure is rather high, then the boundary layer loss is likely to be over-predicted. In fact, comparatively thick boundary layers were computed as can be seen in Fig. 9. This is confirmed by a comparison of the predicted and measured boundary layer integral parameters at the trailing edge. For $M_{2is} = 1.15$, for instance, the predicted displacement thickness amounts to $\delta^* \approx 0.25$ whilst the measured value was of the order $\delta^* = 0.17$, Deckers (1996). The Navier-Stokes predictions show that the inclusion of viscous effects leads to an increase in both base pressure and profile loss and hence confirms the results from the control volume analysis.

The predicted variation of flow exit angle, β_2, as a function of downstream Mach number, M_{2is}, is given in Fig. 13. Both, the

inviscid and viscous method predict slightly higher exit angles compared with the experiments. This is almost certainly due to the fact that fully periodic flow could not be achieved in the tests. However, it should be noted that the discrepancy is less than one degree over the whole Mach number range and that the overall trends are correctly predicted.

Blades with Trailing Edge Ejection

In the following, predictions are presented and compared with experimental results in which the time-marching method was employed to calculate the *inviscid* and viscous transonic flow with coolant ejection from the trailing edge base ($C_{\mu} = 0.5$). A series of computational runs were performed for different isentropic exit Mach numbers, M_{2is}, and coolant flow rates. However, only the results for $M_{2is} = 1.15$ are shown due to the lack of space.

The change in overall flow pattern with increasing coolant flow rate is illustrated in Fig. 14 where contours of Mach number obtained from *inviscid* calculations are plotted. Note, the corresponding prediction without coolant flow is given in Fig. 9. The data show that the flow pattern is easily disturbed by the coolant.

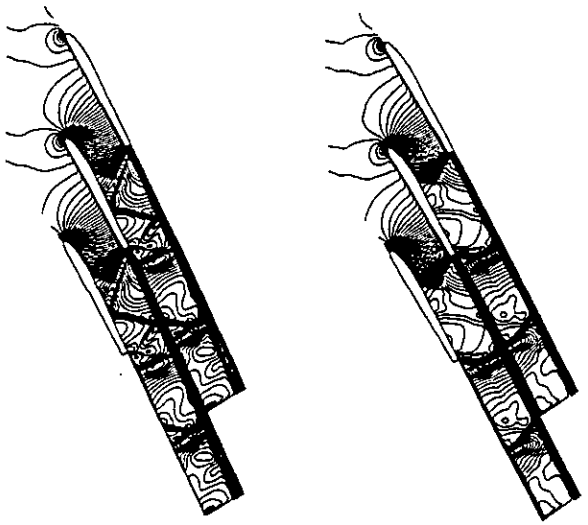

a) $p_{0c} / p_{01} = 0.43$ b) $p_{0c} / p_{01} = 0.62$

Fig. 14: Contours of Mach Number ($M_{2is} = 1.15$)

The predicted and measured surface static pressure distributions for two different coolant flow rates are compared in Fig. 15. At a low coolant flow range, the position of the shock interaction with the suction surface was predicted to be just downstream when compared to the test data. But, at higher ejection rates, the agreement can be seen to be good. Comparisons at different exit Mach numbers showed that the agreement was generally found to improve with increasing ejection rate. It can be seen that the Navier-Stokes and Euler calculations produce very similar results. This illustrates the reduced impact of the shock-boundary layer interaction as the coolant flow increases. For the same reason the agreement between prediction and measurement is seen to improve with increasing bleed.

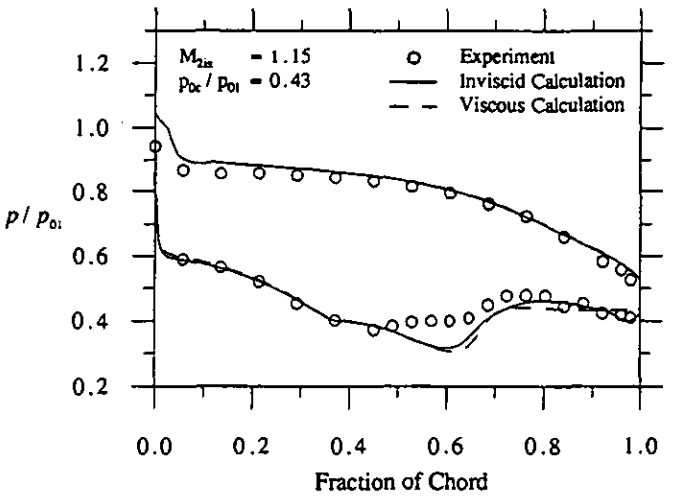

Fig. 15a: Predicted and Measured Surface Static Pressure Variation ($M_{2is} = 1.15$, $p_{0c} / p_{01} = 0.43$)

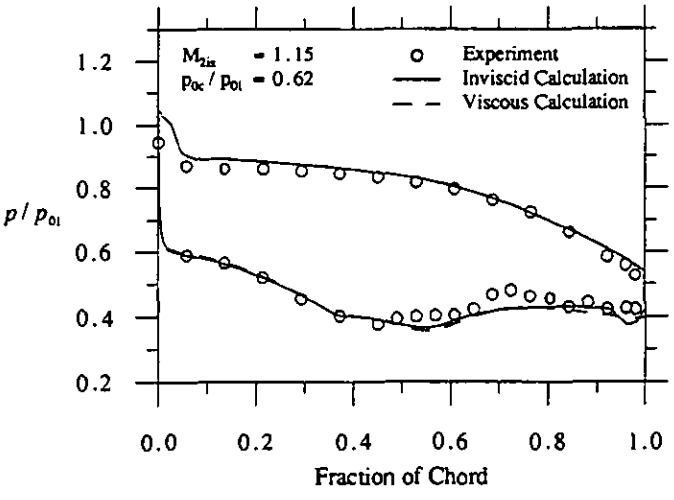

Fig. 15b: Predicted and Measured Surface Static Pressure Variation ($M_{2is} = 1.15$, $p_{0c} / p_{01} = 0.62$)

A comparison between the predicted and measured base pressure variation[8] with coolant flow rate is shown in Fig. 16. Both the *inviscid* and viscous calculations show that the discrepancy observed in base pressure between prediction and experiment for zero bleed ($p_{0c} / p_{b0} = 1$) disappears as the coolant flow is increased. Thus, the numerical calculations correctly predict the overall trends and closely agree with the experimental base pressure values for bleed rates $p_{0c} / p_{b0} \geq 1.5$.

[8] Note that an average value is shown in both cases. The experimentally determined base pressure is the arithmetic mean of the two static pressures measured at each trailing edge partial base (Part 1). Similarly, the calculated value is the arithmetic mean of the predicted average static pressure which is representative for each partial bases.

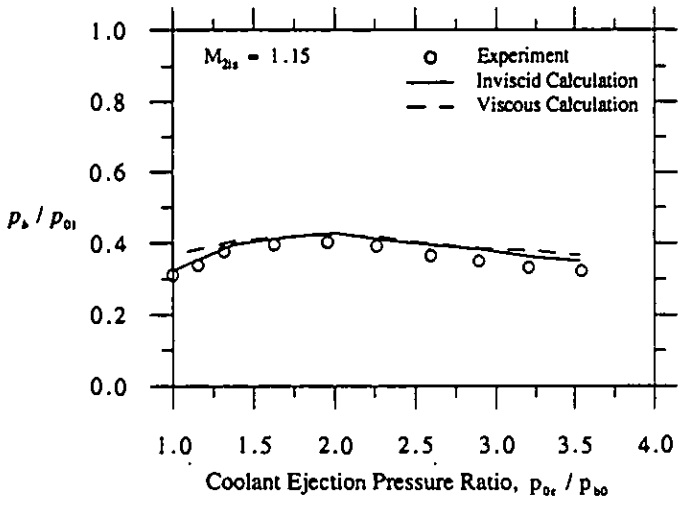

Fig. 16: Predicted and Measured Base Pressures ($M_{2is} = 1.15$)

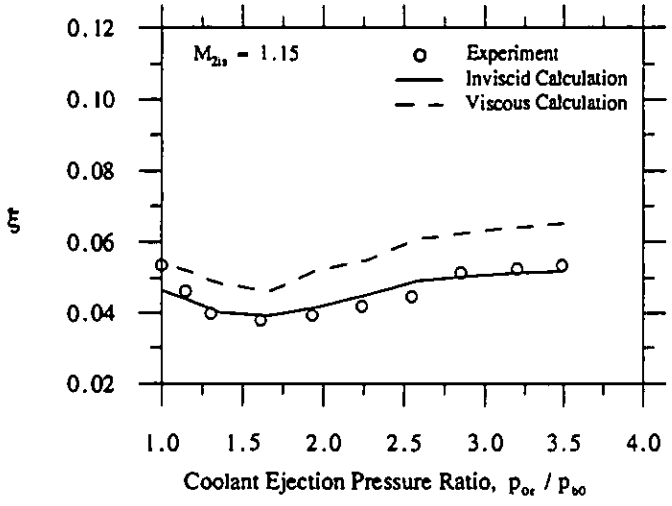

Fig. 17: Predicted and Measured Loss Coefficient ($M_{2is} = 1.15$)

The computed kinetic energy loss coefficient is compared with experimental data in Fig. 17. The *inviscid* results demonstrate that the discrepancy in absolute loss found for zero bleed disappears as the coolant flow increases. In terms of loss level, surprisingly good agreement was achieved. The main reason for this is the fact that both the base pressure and, most importantly, the suction surface pressure distribution were predicted accurately in these cases. As stated above, the trailing edge loss should then be predicted correctly but the viscous loss is not calculated and so the overall loss should be too low. The viscous calculation predicts values for the kinetic energy loss coefficient which are about 1% high compared with the measurements. Hence, the relative reduction in loss due to the coolant flow is underestimated but minimum loss was obtained for an ejection pressure ratio of $p_{0c} / p_{b0} = 1.7$ which is in agreement with the experiments.

Figure 18 shows a comparison between the calculated and measured flow exit angle. The agreement can be seen to improve with increasing coolant bleed. However, the discrepancy is nowhere greater than 1°.

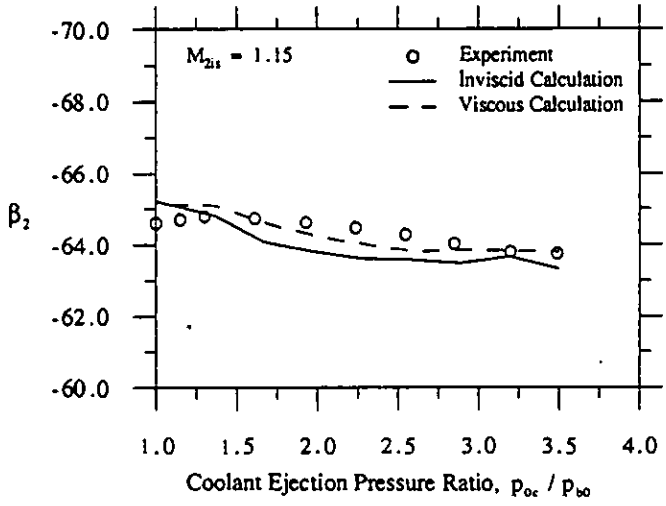

Fig. 18: Predicted and Measured Variation of Exit Flow Angle ($M_{2is} = 1.15$)

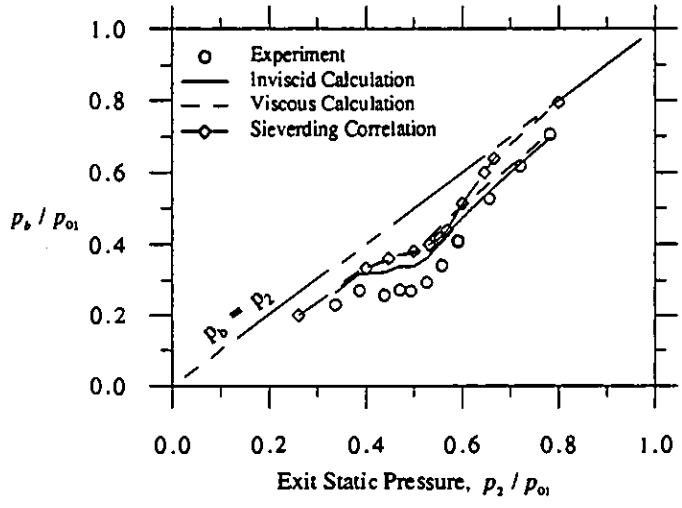

Fig. 19: Predicted and Measured Base Pressure Variation with Exit Static Pressure

CONCLUSIONS

The base pressure and overall loss for unstaggered blades with coolant ejection can be exactly determined by a simple control volume analysis. The agreement between measured and predicted data was found to be very accurate. The theory indicates that for a given coolant ejection pressure ratio the coolant slot should be made as wide as possible and thus confirm that base ejection reduces the effective trailing edge thickness. However, the overall cycle efficiency, of course, is compromised by the coolant.

When interpreting the results, it must be noted that the entire analysis is valid only within the simplifications made above. In practice, the sonic line at the throat ($M_1 = 1$) is likely to be bent due to streamline curvature effects, violating the assumption of uniform flow. Furthermore, in a real turbomachine, a fully mixed-out downstream

flow hardly ever exists. Instead, the trailing edge flow and shock system may have interacted with the downstream blade row well before complete mixing has taken place.

It was shown that the finite volume method is capable of predicting the complex flow that occurs in transonic turbine blading. The results illustrate that the use of a quasi-orthogonal mesh leads to improved modelling of important features, e.g. expansions, shocks, reflections.

The numerical study indicates that the flow through a transonic turbine cascade with and without trailing edge coolant ejection can be computed reasonably well using an *inviscid* Euler code. The results confirm that the overall trends for the base pressure and loss coefficient are calculable without the need to include viscous effects. It is therefore believed that the mechanisms involved can be explained by *inviscid* arguments. The predictions illustrate that good agreement is achieved if the suction surface static pressure distribution is described accurately and, hence, confirm the findings of the global theory.

Good overall agreement was also achieved using the Navier-Stokes solver. The predicted variations of base pressure and loss with isentropic exit Mach number and coolant flow were found to compare well with experimental evidence. However, although reasonable agreement was also obtained for the overall loss level the computed base pressure was generally over-predicted. The predictions confirm that only very little coolant flow ($C_m \approx 1\%$) is necessary to produce a substantial change in the overall flow pattern.

It must be remembered that the calculations are unlikely to be fully grid independent. However, it is very important to realise that despite this they are able to predict the base pressure and loss remarkably well because they satisfy overall conservation as required by the control volume analysis. Hence, better agreement with experimental data was obtained using the present computational method, *inviscid* and viscous, than those derived from Sieverding's (1980) empirical correlation, as shown in Fig. 19. Finally, it should be noted that flow features such as separation bubbles at the location of the shock wave-boundary layer interaction and unsteady vortices downstream of the trailing edge, which were found to be present in the flow, were not computed numerically and, additionally, that numerical errors are inevitable. Given the above limitations, the overall predictive capability of the present method can be concluded to be good.

ACKNOWLEDGEMENTS

The first author was in receipt of a scholarship from the Gottlieb Daimler- und Karl Benz Stiftung and from the Science and Engineering Research Council (SERC). The work was financially supported by the Procurement Executive, Ministry of Defence. Thanks are due to all these organisations.

REFERENCES

Amecke, J. (1970): "Probleme der transsonischen Strömung durch Turbinenschaufelgitter", VDI-Forschungsheft Nr. 540, Düsseldorf, Germany.

Baldwin, B.; Lomax, H. (1978): "Thin Layer Approximation and Algebraic Model for Separated Turbulent Flows", AIAA Paper No. 78-257.

Deckers, M. (1996): "The Influence of Trailing Edge Coolant Ejection on the Loss of Transonic Turbine Blades", Ph.D. Thesis, Department of Engineering, University of Cambridge.

Denton, J.D. (1986): "The Use of a Distributed Body Force to Simulate Viscous Effects in 3D Flow Calculations", ASME Paper No. 86-GT-144.

Denton, J.D. (1982): "An Improved Time Marching Method for Turbomachinery Flow Calculation", ASME Paper No. 82-GT-239.

Denton, J.D. (1993): "Loss Mechanisms in Turbomachines", ASME Paper No. 93-GT-435.

Denton, J.D.; Xu, L. (1989): "The Trailing Edge Loss of Transonic Turbine Blades", ASME Paper No. 89-GT-278.

Hartsel, J.E. (1972): "Prediction of Effects of Mass-Transfer Cooling on the Blade Row Efficiency of Turbine Airfoils", AIAA Paper No. 72-11.

Lakshminarayana, B. (1991): "An Assessment of Computational Fluid Dynamic Techniques in the Analysis and Design of Turbomachinery - The 1990 Freeman Scholar Lecture", Journal of Fluids Engineering, Vol. 113, p. 315.

Lieblein, S.; Roudebush, W.H. (1956): "Theoretical Loss Relations for Low-Speed Two-Dimensional Cascade Flow", NACA TN 3662.

Martelli, F.; Michelassi, V.; Boretti, A.A. (1992): "Numerical Modelling of Coolant Jet Flow in Turbine Cascades", Bulletin S.F.M., Revue Française des Mécanique n° 1992-4.

Michelassi, V.; Martelli, F.; Amecke, J. (1994): "Aerodynamic Performance of a Transonic Turbine Guide Vane with Trailing Edge Coolant Ejection", Part 2: Numerical Approach, ASME Paper No. 94-GT-248.

Ni, R.-H.; Bogoian, J. C. (1989): "Prediction of 3D Multi-Stage Turbine Flow Field using a Multiple-Grid Euler Solver", AIAA Paper No. 89-0203.

Prust, H.W. (1972): "An Analytical Study of the Effect of Coolant Flow Variables on the Kinetic Energy Output of a Cooled Turbine Blade Row", AIAA Paper No. 72-12.

Schlichting, H. (1968): "Boundary Layer Theory", Sixth Edition, McGraw-Hill.

Schobeiri, T. (1989): "Optimum Trailing Edge Ejection for Cooled Gas Turbine Blades", ASME Journal, Vol. III, pp. 510-514.

Sieverding, C.H.; Stanislas, M.; Snoek, J. (1980): "The Base Pressure Problem in Transonic Turbine Cascades", ASME Paper No. 79-GT-120.

Stewart, W.L. (1955): "Analysis of Two-Dimensional Compressible-Flow Loss Characteristics Downstream of Turbomachine Blade Rows in Terms of Basic Boundary Layer Characteristics", NACA TN 3515.

Turner, M.G.; Liang, T.; Beauchamp, P.P.; Jennions, I.K. (1993): "The Use of Orthogonal Grids in Turbine CFD Computations", ASME Paper No. 93-GT-38.

Xu, L. (1985): "The Base Pressure and Trailing Edge Loss of Transonic Turbine Blades", Ph.D. Thesis, Department of Engineering, University of Cambridge.